Mixing Polyaromatic Scaffolds and Main Group Elements: Synthesis, Coordination and Optical Properties of Naphthyl-Fused Heteropines.

Thomas Delouche, Thierry Roisnel, Vincent M Dorcet, Muriel Hissler, Pierre-Antoine Bouit

Mixing Polyaromatic Scaffolds and Main Group Elements: Synthesis, Coordination and Optical Properties of Naphthyl-Fused Heteropines

Thomas Delouche, Thierry Roisnel, Vincent Dorcet, Muriel Hissler* and Pierre-Antoine Bouit*

Dr T. Delouche, Dr T. Roisnel, Dr. V. Dorcet, Prof. M. Hissler, Dr. P-A. Bouit
Univ. Rennes, CNRS, ISCR - UMR 6226, F-35000 Rennes
E-mail : muriel.hissler@univ-rennes1.fr, pierre-antoine.bouit@univ-rennes1.fr

Dedicated to J.-R. Hamon on the occasion of his 65th birthday

TABLE OF CONTENT

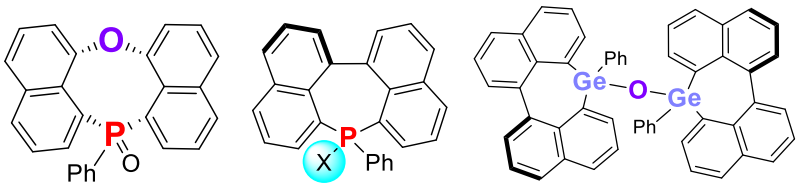

X: =O, Au(I), Pd(II)...

Distorted π-systems featuring main group elements

Polyaromatic 7-membered rings featuring main group elements (P, Ge) are described. Coordination complexes were synthesized with the trivalent phosphepines highlighting that these P-heterocycles are promising ligands. Furthermore, those polyaromatic germepines and phosphepines appear as interesting building blocks for optoelectronics.

ABSTRACT

In this article, we describe the synthesis of polyaromatic heteropines including main group element (Phosphorus, Germanium) through Ni or Cu-mediated C-C coupling. Coordination complexes were synthesized with the σ^3,λ^3-phosphepines using different metal ions (Au(I), Re(I), Pd(II)) showing that these P-heterocycles display the classical reactivity of two-electrons P-donor making them promising ligands. The optical properties were experimentally studied (UV-vis absorption and emission) and compared. Finally, both polyaromatic germepine and phosphepine appear as interesting building blocks for optoelectronics.

INTRODUCTION

Polycyclic Aromatic Hydrocarbons (PAHs) have been attracting attention since decades but the discovery of graphene prompted the scientific community to intensify the study of graphene molecular analogs (also called nanographenes). These organic compounds are composed of sp^2-C atoms and can be planar or distorted. Their particular structure confers them unique properties in term of reactivity, optical/redox activity, self-assembly and opto-electronic device performances.[1] They are thus an important class of organic semi-conductors. A strategy to modify the properties of PAHs is to switch from benzenoids structures to compounds featuring various ring sizes[2] or to introduce heteroatoms (O, S, N, B, P, Si ...).[3] Both strategies can also be combined. In this context, the synthesis of heteropines (7-membered heterocycles featuring heteroelement) recently appeared as an appealing strategy.[4] For example various naphthyl-fused heteropine incorporating oxygen **A**[5], boron **B**[6], nitrogen **C**[7] or phosphorus **D**[8] have been described in the last years (Scheme 1). All these π-extended heteropines display a strongly distorted C-framework and can be emissive in solution. The insertion of the heteroatom allows modifying the molecular distortion and tuning the optical properties. In the present article, we detail the molecular engineering and the reactivity of our recently reported naphthyl-fused phosphepine.[8] As an extension of the synthetic strategy, the synthesis of germanium-containing heteropine (germepine) was investigated (Scheme 1). Furthermore, we report on a detailed study on the optical properties of the phosphepine and germepine.

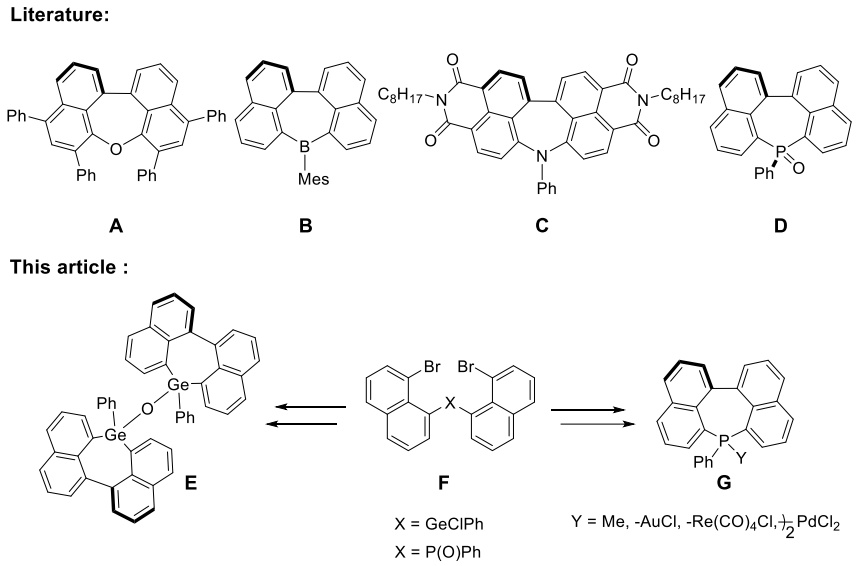

Scheme 1. Naphtyl-fused heteropines described in the literature: Oxepine (**A**), Borepine (**B**), Azepine (**C**), Phosphepine (**D**) and synthetic strategy developed in this article.

RESULTS AND DISCUSSION.

The phosphepine **3** can be synthesized through a Yamamoto coupling involving Ni-coupling on the dibromonaphtylphenylphosphine oxyde **1** (Scheme 2).[8],[9] Since this reaction is very air and moisture sensitive, we tested an Ullmann coupling, another well-known strategy to realize C-C coupling.[10] The advantage of this pathway is the use of Cu(0) which is less air and moisture sensitive than Ni(0). This approach was tested on **1** in classical Ullman conditions (Cu(0), DMF). This methodology surprisingly led to the formation of the phosphocine **2** (Scheme 2), an 8-membered ring including a phosphorus and an oxygen atom. [11] The most favorable explanation of this compound formation would be the presence of water traces in the media. Indeed, adding water in the media, allowed increasing the yield until 35%. Interestingly, the Ullmann coupling leads to the 8-membered ring (**2**) only with the precursor with the exocyclic P-Ph bond (**1**). When the P-atom is substituted with alkoxy or aryloxy (**4**, **5**, Scheme 2), the Ullmann coupling leads to the formation of seven-membered rings: phosphepine **6** and **7** (Scheme 2). However the yields are smaller compared to the Yamamoto coupling involving Ni-coupling (Scheme 2). All compounds were fully characterized by means of multinuclear NMR spectroscopy and mass spectrometry.

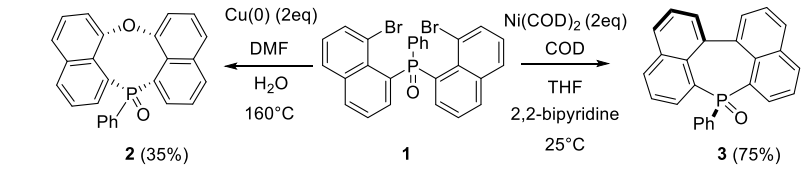

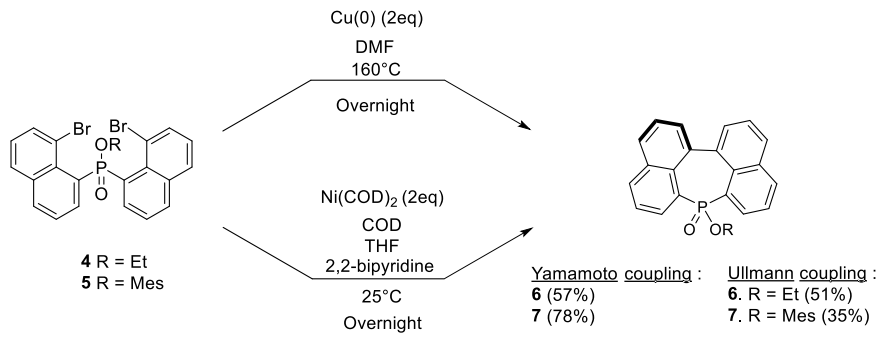

Scheme 2. Ullmann and Yamamoto coupling on the precursor **1**, **4-5** leading to the phosphocine **2** and the phosphepines **3**, **6-7**

Phosphocine **2** was characterized by X-ray diffraction (Figure 1 and Table S1-S2). The X-ray structure shows that the 8-membered ring **2** adopts a bended structure with an angle between the naphthyl groups of 121.87° and non-bonding peri-distance d(O**…**P) = 2.79 Å, in the range of previously reported P,O peri-substituted naphthalenes.[12] It is worth mentioning that the two naphthyl groups keep their planarity. On the contrary, the 7-membered ring **3** adopts a twisted structure with a torsion angle between the naphthyl groups of 35.80°.[8] As for the phosphepine, the P-C bonds lengths are classical for phosphine-like structures ($d_{P\text{-}C}$ = 1.79-1.80 Å). In the 8-membered P-ring, all C-C bonds belonging to the naphthalene moiety are within the aromatic C-C distances (1.41 Å< d< 1.44 Å). The C-O bonds also display classical distances (1.39 Å< d< 1.40 Å).

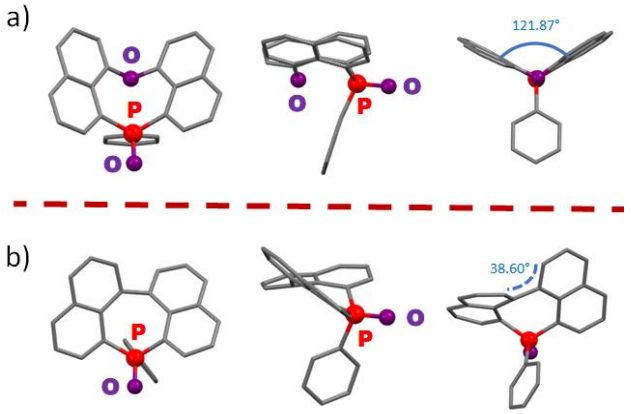

Figure 1. Top (left), lateral (center) and back (right) crystallographic views of **2** (a) and **3 (**b).

With the naphthyl-fused phosphepine oxide **3** in hands, we were interested in testing whether this P-atom locked in a distorted P-heterocycle remains reactive. Thus, the phosphorus atom of compound **3** was deprotected by a reductive treatment with $HSiCl_3$ allowing to obtain the σ^3,λ^3-phosphepine **8**. Then, this intermediate was directly reacted with MeOTf to afford cationic derivative **9** or with various metallic ions to afford quantitatively coordination complexes **10** with Au(I), **11** with Re(I) and **12** with Pd(II)(Scheme 3). All compounds were fully characterized by means of multinuclear NMR spectroscopy and mass spectrometry and complexes **10** and **12** were additionally characterized by X-ray diffraction (*vide infra*). This study shows that naphthyl-fused phosphepines display the classical reactivity of σ^3,λ^3-phosphane which allows to easily diversify its molecular structures.

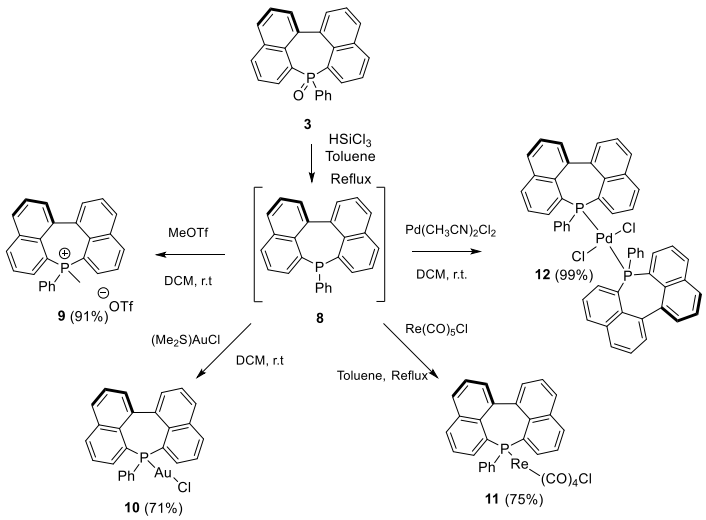

Scheme 3. Synthesis of the naphthyl-fused phosphepinium **9** and the phosphepine complexes **10**-**12**.

Complexes **10** and **12** were characterized by single-crystal X-ray diffraction. In the X-ray structure of **10** and **12**, metric parameters of the polycyclic framework of the phosphepine ligand are similar to those of the previously reported phosphepine **3** (Table S3).[8] Complex **10** crystallizes in the *P-1* space group of the triclinic system (Table S1). In this derivative, the P-center of the ligand L acts as expected, as a two-electron donor toward the Au(I) metal center (d(P-Au), 2.246 Å) and the P-Au-Cl fragment is almost linear (P-Au-Cl, 177.1°). Complex **12** crystallizes in the P 2_1/n space group of the triclinic system (Table S1). The P-Pd bond lengths are classical for a phosphine σ^3-P center acting as two electron donor on a Pd(II) metal center (d(P-Pd), 2.327) Å.Furthermore, a distorted square planar geometry is observed around the Pd(II) ion (87.8° < P-Pd-Cl < 92.2°) with the two P-ligands coordinated on *trans*-position and the P-Ph in *trans* of the P-Pd-P fragment (Fig. 2). This situation markedly differs compared to our previously reported Pd-complex featuring two planar P-containing PAH ligands in which intra-complex π-stacking induced an unconventional *cis*-conformation.[13] The present behavior can be attributed to the distorted π-surface of the ligand **8** which prevent inter-ligands interactions. Furthermore, the distorted phosphepine backbone also prevents inter-complexes interactions. Based on those examples, the rich coordination chemistry of phosphine can be transposed to naphthyl-fused phosphepine, which contrasts with Lammerstma's σ^3,λ^3-P-diphenylphosphepine which acted as heterobidentate phosphane-olefin ligands, due to the presence of a double bond with an olefinic character.[14]

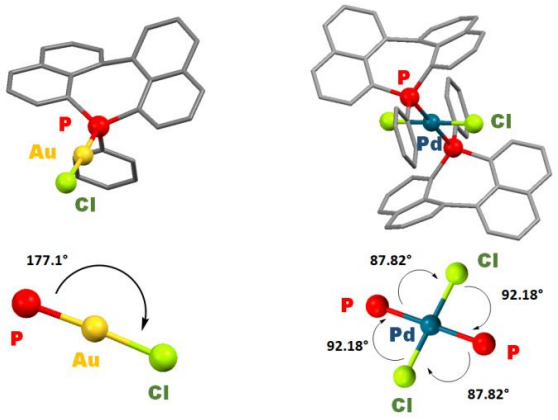

Figure 2. Crystallographic structures of **10** (left) and **12** (right) and zoom on the metal environments (Bottom).

To modify the nature of the heteroatom within a π-extended-heteropine, we decided to use the Ni-mediated coupling strategy for the synthesis of group 14 containing heteropines. After various unsuccessful tests with silane derivatives, we developed a synthetic strategy toward naphthyl-fused germepines (Scheme 1 and 4).
First, a lithiation was realized on the 1,8-dibromonaphthalene. Then, the lithiated compound was reacted with phenyltrichlorogermane leading to the formation of the **13.** Despite the presence of broad signals in ^{1}H NMR, this compound was unambiguously characterized by its crystallographic structure (Figure 3). The treatment with KOH allowed obtaining the intermediate **14** with a Ge-O-Ge bond.[15] Finally, **14** was reacted in the Yamamoto conditions (2 equivalent of Ni(COD)$_2$, COD and 2,2-bipyridine) to afford **15** with good yields (60%) (Scheme 3). This compound is composed of two naphthyl-fused germepines linked through a Ge-O-Ge bond.

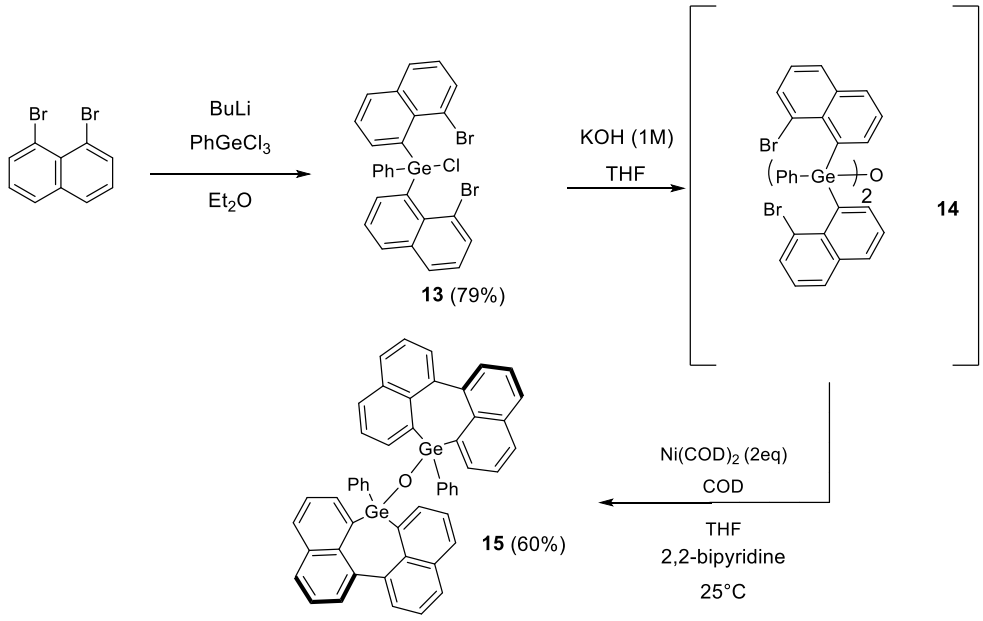

Scheme 4. Synthesis of **15**

The fluxional character observed in NMR for **13** can be explained by the presence of interconverting rotamers around the germanium atom at room temperature as already observed for B- and P-analogues.[6],[8] Indeed, the ^{1}H NMR signals sharpened upon cooling to 223K (Figure S6). Moreover, the chemical stability of the chlorogermane **13** can be explained by the steric protection afforded by the bulky bromonaphthyl and in particular the presence of short distances between the peri-substituted Br and Ge (3.104 Å<d_{GeBr}< 3.262 Å; d_{VdW}(Ge-Br) = 3.96 Å, Figure 3). The same behaviour was observed with the phosphine oxide **1**.[8]

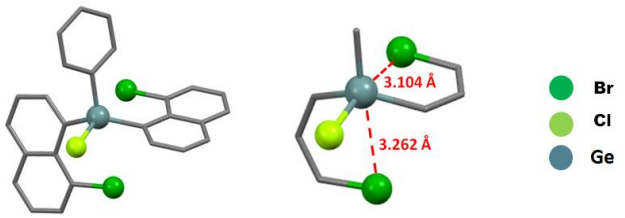

Figure 3. Depictions of the X-ray crystal structures of **13** with zoom on the Ge environment with measured Ge-Br distances (red dotted line) (right).

The optical properties of all compounds were investigated in dichloromethane (C = 10^{-5}M). The absorption spectrum of the naphthyl-fused phosphepine 3 consists of a large band (λ_{abs} = 346 nm) associated with a π-π* transition.[8] The compound also displays a blue luminescence centered at 446 nm. First, the impact of P-functionalization was investigated with the cationic phosphepine **9** and complexes **10**-**12**. The optical properties (both absorption and emission spectra) of these compounds are similar to those of phosphepine oxide **3** (see Figure S13). Hence, we already showed that the phosphorus atom is not involved in the MOs linked with the π–π* transitions, which explains the weak impact on the optical properties of the modification performed at the phosphorus atom.[8] Such behavior was also observed on π-extended phosphepine with different backbone.[16]

Then, the impact of the molecular structure between phosphocine **2** and phosphepine **3** was investigated. Phosphocine **2** displays an absorption band in the UV region centered at 304 nm. (Fig. 4, Table 1). Compared with phosphepine **3**, the insertion of an oxygen atom leads to a hypsochromic shift of 42 nm (λ_{abs}(**2**): 304 nm and λ_{abs}(**3**): 346 nm). This observation is in accordance with the disruption of the conjugation induced by the presence of the O-atom within the π-framework together with the large angle between the two naphthalenes (121.9°, Fig. 1). Despite this conjugation disruption, compound **2** also displays a luminescence centered at 355 nm which is hypsochromically shifted by 91 nm

compared to the emission of compound **3** (λ_{em} = 446 nm). Furthermore, a smaller Stokes shift (σ(**2**): 4726 cm^{-1} < σ(**3**): 6480 cm^{-1}) is observed for compound **2** indicating a smaller reorganization in the excited state. These observations show that the emission properties originates mainly from the substituted naphthalenes.[17]

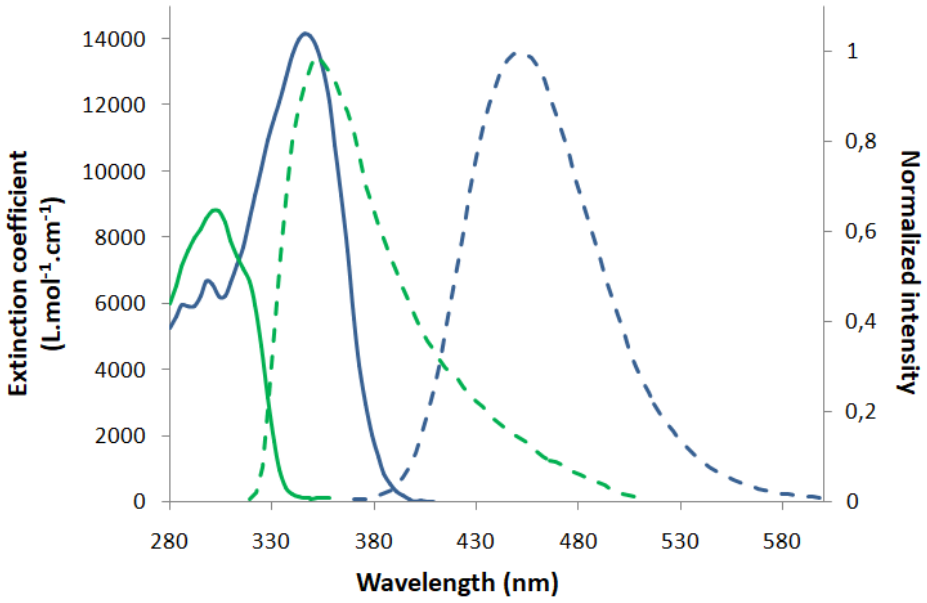

Figure 4. UV–vis absorption (continuous line) and emission (dot line) of **2** (Green) and **3** (Blue) in diluted DCM (C = 10^{-5}M)

To further study the impact of the heteroatom insertion within the heteropine scaffold, the phosphepine **3** and the germepine **15** UV-Vis absorption and fluorescence spectra were compared (Figure 4). Germepine **15** displays an absorption band in the UV region (λ_{max}(**15**): 319 nm). The presence of the germanium atom leads to a 27 nm hypsochromic shift in absorption compared to phosphepine **3**. A weak bathochromic shift is observed in emission (λ_{em}(**3**): 446 nm and λ_{em}(**15**): 457 nm). The Stokes shift with Ge is thus increased compared to P (σ(**3**): 6480 cm^{-1} and (σ(**15**): 9466 cm^{-1}) which means that there is a stronger reorganization in the excited state for this species. If we compare with the boron analog **B** (Figure 1), (σ(**B**)= 1360 cm^{-1}),[6] there is clearly a link between the heteroatom nature and the Stokes shift. Thus, a longer Heteroatom-C bond ($d_{B\text{-}C}$<$d_{P\text{-}C}$<$d_{Ge\text{-}C}$) leads to stronger reorganization in the excited state.

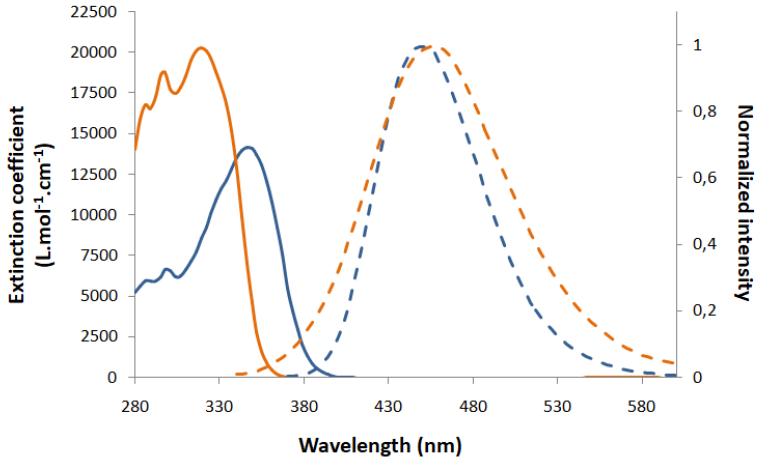

Figure 4. UV–vis absorption (continuous line) and emission (dot line) of **3** (blue) and **15** (Orange) in diluted DCM (C = 10^{-5}M)

Table 1: Photophysical data.

Compound	λ_{abs} (nm)[a]	λ_{em} (nm)[a]	σ (cm^{-1}) [a]	ε_{max} ($L.mol^{-1}.cm^{-1}$)[a]	Φ[b]
2	304	355	4726	8830	0.06
3	346	446	6480	14160	0.46
9	351	454	6464	12800	0.22
10	351	454	6464	9600	0.05
11	339	452	7375	13200	0.03
12	347	447	6447	20100	<0.01
15	319	457	9466	20300	0.27

[a] In CH_2Cl_2 (10^{-5}M). [b] Quantum yield measured relative to quinine sulfate (H_2SO_4, 1 N), ϕ_{ref}= 0.55.

CONCLUSIONS

In conclusion, the synthesis of various heteropines featuring P or Ge atoms is described (**3**, **12**), as well as the unexpected preparation of a phosphocine (**2**). The reactivity of the σ^3,λ^3-P-heteropine **4** is similar to classical phosphine, in particular for its coordination chemistry. Then, the germanium analogue of the phosphepine has been synthesized through an unusually stable chlorogermane precursor. The effect of the ring structure (phosphepine vs phosphocine) and of the heteroatom nature (P *vs* Ge) was studied through optical spectroscopy highlighting that both the ring size and the nature of the main group element impact the absorption and luminescence properties. This study confirms the potential of π-extended heteropine for potential optoelectronic applications and paves the way toward the preparation of heavier main group elements containing PAHs.[18]

Experimental Section

All experiments were performed under argon atmosphere using standard Schlenk techniques. Commercially available reagents were used as received without further purification. Solvents were freshly purified using MBRAUN SPS-800 drying columns. Separations were performed by gravity column chromatography on basic alumina (Aldrich, Type 5016A, 150 mesh, 58 Å) or silica gel (Merck Geduran 60, 0.063-0.200 mm). ^{1}H, ^{13} C, and ^{31}P NMR spectra were recorded on Bruker AV III 300 and 400 MHz NMR spectrometers equipped with BBO or BBFO probeheads. Assignment of proton and carbon atoms is based on COSY, NOESY, edited-HSQC and HMBC experiments. ^{1}H and ^{13}C NMR chemical shifts were reported in parts per million (ppm) using residual solvent signal as reference. In the NMR description. High-resolution mass spectra were obtained on a Varian MAT 311 or ZabSpec TOF Micromass instrument at CRMPO (Scanmat, UMS 2001). UV-Visible spectra were recorded rt on a VARIAN Cary 5000 spectrophotometer. The UV-Vis, emission and excitation spectra measurements were recorded on a FL 920 Edinburgh Instrument equipped with a Hamamatsu R5509-73 photomultiplier for the NIR domain (300-1700 nm) and corrected for the response of the photomultiplier. Quantum yields in solution were calculated relative to quinine sulfate (H_2SO_4, 0.1 M), ϕ_{ref}= 0.55. **1** and **3** were synthesized according to published procedures.[8] **6-7** were synthesized according to general method A (without addition of water) and their NMR data fit with our previously reported synthesis.[8] CCDC 1913087 (**2**)-1913089 (**10**), 1913090 (**12**), 1974630 (**13**) contains the supplementary crystallographic data for this paper. These data can be obtained free of charge from The Cambridge Crystallographic Data Centre.

2 (General method A). **1** (200 mg, 0.37 mmol, 1 eq) and Cu(0) (47 mg, 0.75 mmol, 2 eq) are dissolved in 30 mL of DMF and 1 mL of water is added. Then the reaction is heated to 160°C during 2 day. Then DMF is evaporated and the crude mixture was purified by silica gel chromatography using DCM/AcOEt (1/1) to afford **2** as a white powder (49 mg, 35 %).^{1}H NMR (400 MHz, CD_2Cl_2) δ 9.00 (ddd, 2H, *J* = 14.5, 7.2, 1.3 Hz, H_8), 8.10 (d, 2H, *J* = 8.2 Hz, H_6), 7.81 (d, 2H, *J* = 8.2 Hz, H_4), 7.76 (t, 2H, *J* = 8.1 Hz, H_7), 7.66 (d, 2H, *J* = 7.7 Hz, H_2), 7.53 (t, 2H, *J* = 7.9 Hz, H_3), 7.41 – 7.34 (m, 1H, H_{para}), 7.29 – 7.16 (m, 4H, $H_{meta,\ ortho}$). ^{13}C NMR (101 MHz, CD_2Cl_2) δ 154.85 (d, *J* = 2.8 Hz, C_q), 139.38 (d, *J* = 121.7 Hz, C_{ipso}), 137.26 (d, *J* = 6.5 Hz, C_8), 135.49 (d, *J* = 8.0 Hz, C_q), 132.81 (d, *J* = 3.0 Hz, C_6), 130.52 (d, *J* = 2.9 Hz, C_{para}), 129.08 (d, *J* = 5.5 Hz, C_q), 128.77 (d, *J* = 13.7 Hz, C_{ortho}), 128.30 (d, *J* = 11.1 Hz, C_{meta}), 126.99 (C_3), 126.78 (d, *J* = 12.8 Hz, C_7), 126.58 (d, *J* =

101.4 Hz, C_9), 126.43 (d, J = 1.4 Hz, C_4), 118.99 (C_2). ^{31}P NMR (162 MHz, CD_2Cl_2) δ + 25.8. (ESI, CH_3OH/DCM) : $[M+Na]^+$: m/z calculated : 415.0864, found : 415.0858

9. (General method B) **2** (80 mg, 0.2 mmol, 1 eq) is dissolved in 6 mL of dry toluene. $HSiCl_3$ (270 mg, 2.0 mmol, 10 eq) is added dropwise and then heated to reflux 1h. The mixture is filtered on alumina under argon and wash with distillated THF. The solvent is evaporated under the schlenk line vacuum and the resulting intermediate **8**[9a] is dissolved in 10 mL of dry DCM, then MeOTf (98 mg, 0.6 mmol, 3 eq) is added to 0°C. The mixture is stirred at R.T. for 1h30 and finally washed with an extraction H_2O/DCM. The organic phase is dried on $MgSO_4$ and the solvent evaporated. A minimun of DCM is used to dissolve the mixture, heptane is added and the flask is put in fridge during 1 night. The next day the solvent is removed to afford **9** as a white powder. (95 mg, η = 91 %). ^{1}H NMR (400 MHz, CD_2Cl_2) δ 8,38 (dt, 2H, J = 8.2 Hz, J = 1.6 Hz, H_6), 8.09 (m, 4H, H_8 et H_{2or4}), 7.79 (m, 2H, H_7), 7.73 (t, 2H, J = 7.7 Hz H_3), 7.63 (m, 1H, H_{para}), 7.58 (m, 2H, H_{2or4}), 7.45 (m, 2H, H_{meta}), 7.21 (m, 2H, H_{Ortho}), 2.64 (m, 3H, H_{13}). ^{13}C NMR (101 MHz, CD_2Cl_2) δ 138.4 (d, J_{C-P} = 2.9 Hz, C_q), 138.2 (s, C_{2or4}), 137.3 (d, J_{C-P} = 3.4 Hz, C_6), 136.4 (d, J_{C-P} = 9.6 Hz, C_{2or4}), 135.0 (d, J_{C-P} = 3.0 Hz, C_{para}), 134.3 (d, J_{C-P} = 10,4 Hz, C_q), 132.9 (d, J_{C-P} = 9.1 Hz, C_q), 132.3 (d, J_{C-P} = 10.7 Hz, C_{ortho}), 131.2 (d, J_{C-P} = 1.6 Hz, C_8), 130.4 (d, J_{C-P} = 13.1 Hz, C_{metha}), 128.6 (s, C_3), 126.2 (d, J_{C-P} = 14.5 Hz, C_7), 122.9 (d, J_{C-P} = 91.6 Hz, C_{ipso}), 114.8 (d, J_{C-P} = 86.3 Hz, C_9), 12.6 (d, J_{C-P} = 61.3 Hz, C_{13}). ^{19}F NMR (376 MHz, CD_2Cl_2): δ -79.9 (s) ^{31}P NMR (162 MHz, CD_2Cl_2) δ + 23.7. HRMS (ESI, CH_3OH / CH_2Cl_2: 90/10) M^+(C_{27} H_{20} P) : m/z Calculated : 375.12971, m/z Found : 375.1298.

10. General method B was used with **2** (60 mg, 0.153 mmol, 1 eq), 5 mL of dry toluene, $HSiCl_3$ (207 mg, 1.53 mmol, 10 eq) and Me_2SAuCl (45 mg, 0.153 mmol, 1 eq). The compound is dissolved in DCM and filtered on celite. Then heptane is added and the flask is put in the fridge during 1 night. The next day the solvent is removed to afford the compound **10** as a white powder (64 mg, η = 71 %). ^{1}H NMR (400 MHz, CD_2Cl_2) δ 8,82 (ddd, 2H, J = 21.6 Hz, J = 6.9 Hz, J = 1.3 Hz, H_8), 8.13 (d, 2H, J = 8.3 Hz, H_6), 7.90 (d, 2H, J = 8.1 Hz, H_{2or4}), 7.68 (t, 2H, J = 6.8 Hz H_7), 7.50 (t, 2H, J = 7.6 Hz, H_3), 7.34 (d, 2H, J = 7.4 Hz, H_{2or4}), 7.07 (m, 1H, H_{para}), 6.93 (m, 2H, H_{meta}), 6.54 (m, 2H, H_{Ortho}). ^{13}C NMR (101 MHz, CD_2Cl_2) δ 140.9 (d, J_{C-P} = 27.6 Hz, C_8), 139.3 (d, J_{C-P} = 2.3 Hz, C_q), 136.6 (s, C_{2ou4}), 134.7 (d, J_{C-P} = 2.9 Hz, C_6), 134.4 (d, J_{C-P} = 7.1 Hz, C_q), 133.8 (d, J_{C-P} = 60,4 Hz, C_{ipso}), 133.7 (d, J_{C-P} = 3.4 Hz, C_q), 130.9 (d, J_{C-P} = 12.7 Hz, C_{ortho}), 130.5 (d, J_{C-P} = 2.6 Hz, C_{para}), 130.3 (d, J_{C-P} = 0.9 Hz, C_{2or4}), 128.5 (s, C_{meta}), 127.3 (s, C_3), 125.3 (d, J_{C-P} = 17.9 Hz, C_7), 124.1 (d, J_{C-P} = 60.1 Hz, C_9). ^{31}P NMR (162 MHz, CD_2Cl_2) δ + 45.7. HRMS (ESI, CH_3COCH_3) $[M+Na^+]$(C_{26} H_{17} ^{35}Cl Na P Au) : m/z Calculated : 615.03142 m/z Found : 615.0316.

11. General method B was used with **2** (80 mg, 0.204 mmol, 1 eq), 5 mL of dry Toluene and $HSiCl_3$ (275 mg, 2.04 mmol, 10 eq). After the phosphorus deprotection, the mixture is dissolved in 10 mL of dry Toluene and $Re(CO)_5Cl$ (73 mg, 0.204 mmol, 1 eq) is added. Then the mixture is heated to reflux during 1h30. Finally the compound is dissolved in DCM and filtered on celite. Then heptane is added and the flask is put in the fridge during 1 night. The next day the solvent is removed to afford the compound **11** as a white powder (106 mg, η = 75 %). ^{1}H NMR (400 MHz, CD_2Cl_2) δ 7.98 (m, 6H), 7.65 (t, 2H, J = 7.6 Hz), 7.58 (m, 3H), 7.51 (m, 2H, H_{meta}), 7.41 (m, 4H). ^{13}C NMR (101 MHz, CD_2Cl_2) δ 186.2 (d, J_{C-P} = 8.6 Hz, C_{CO}), 184.6 (d, J_{C-P} = 58.4 Hz, C_{CO}), 182.5 (d, J_{C-P} = 5.1 Hz, C_{CO}), 140.4 (d, J_{C-P} = 2.6 Hz, C_q), 137.0 (d, J_{C-P} = 2.3 Hz, CH), 136.6 (s, CH), 135.2 (d, J_{C-P} = 49.4 Hz, C_{ipso}), 135.1 (d, J_{C-P} = 12.3 Hz, CH), 134.3 (d, J_{C-P} = 7.6 Hz, C_q), 132.4 (d, J_{C-P} = 2.8 Hz, CH), 132.3 (d, J_{C-P} = 7.4 Hz, C_q), 132.0 (d, J_{C-P} = 2.4 Hz, CH), 131.5 (d, J_{C-P} = 45.5 Hz, C_9), 131.0 (s, CH), 129.4 (d, J_{C-P} = 10.4 Hz, C_{meta}), 127.3 (s, CH), 125.5 (d, J_{C-P} = 12.3 Hz, CH). ^{31}P NMR (162 MHz, CD_2Cl_2) δ + 15.2. HRMS (ESI, CH_2Cl_2): $[M-Cl]^+$(C_{30} H_{17} O_4 P Re) : m/z Calculated : 659.0422, m/z Found : 659.0414

12. General method B was used with **2** (60 mg, 0.153 mmol, 1 eq), 5 mL of dry Toluene, $HSiCl_3$ (207 mg, 1.53 mmol, 10 eq) and $Pd(CH_3CN)Cl_2$ (18 mg, 1.53 mmol, 10 eq). The compound is dissolved in DCM and filtered on celite. Then heptane is added and the flask is put in the fridge during 1 night. The next day the solvent is removed to afford the compound **12** as a yellow powder (61 mg, η = 97 %). ^{1}H NMR (400 MHz, CD_2Cl_2) δ 8.80 (q, 4H, J = 8.2 Hz, H_8), 8.10 (t, 4H, J = 8.2 Hz, H_6), 7.92 (d, 4H, J = 8.0 Hz, H_7), 7.71 (t, 2H, J = 7.5 Hz, H_{2or4}), 7.53 (t, 4H, J = 7.6 Hz, H_7), 7.38 (d, 4H, J = 7.4 Hz, H_{2or4}), 7.12 (t, 2H, J = 8.1 Hz, H_{para}), 7.01 (t, 4H, J = 7.6 Hz, H_{meta}), 6.81 (m, H_{ortho}). ^{13}C NMR not measured for solubility reasons ^{31}P NMR (162 MHz, CD_2Cl_2) δ + 36.2.HRMS (ESI, CH_3COCH_3) $[M+Na^+]$(C_{52} H_{34} Cl_2 Na P_2 Pd) : m/z Calculated : 921.0444, m/z Found : 921.0439.

13. 1,8-Dibromonaphtalene (1.0 g, 3.53 mmol, 2.7 eq) is dissolved in 50 mL of dry Et_2O. The solution is cooled down to -80°C then BuLi (1.41 mL, 3.53 mmol, 2.7 eq) is added dropwise and the solution is stirred for 30 mn at -80°C then 30 mn at rt. The solution is again cooled down to -80°C and $PhGeCl_3$ (120 mg, 0.47 mmol, 1 eq) is added dropwise. The mixture is then stirred at RT overnight. Then the solution is extracted with water and the organic phase is dried on $MgSO_4$ and evaporated. The crude mixture is purified by silica gel chromatography using DCM/C_7 (1/1). The compound is dissolved in a minimum of DCM and heptane is added. The flask is put in the fridge during 1 night. The next day the solvent is removed to afford the compound **13** as colorless crystals (0.580 mg, η = 79%). ^{1}H NMR (400 MHz, CD_2Cl_2, 223K) δ 8.83 – 8.68 (m, 1H), 8.05 – 7.86 (m, 5H), 7.79 – 7.70 (m, 2H), 7.67 – 7.56 (m, 3H), 7.48 – 7.28 (m, 6H). ^{13}C NMR

(101 MHz, CD_2Cl_2, 230K) δ 142.87, 140.45, 136.30, 136.26, 135.87, 135.84, 132.06, 131.72, 131.30, 131.16, 131.04, 129.66, 129.51, 129.45, 127.85, 126.61, 126.44, 126.36, 125.55, 122.35, 121.95. HRMS : (ESI, CH_2Cl_2/CH_3OH : 9/1) $[M+Na^+](C_{26}H_{17}ClBr_2NaGe_2)$: m/z Calculated : 618.84895, m/z Found : 618.8489.

15. **10** (100 mg, 0.167 mmol, 1 eq) is dissolved in 5 mL of THF and 5 mL of NaOH (1M) are added. The mixture is stirred during 1h. Then an extraction DCM/H_2O is realized, the organic phase is dried on $MgSO_4$, filtered on cotton and the solvent is evaporated to afford intermediate **14** (HRMS : (ESI, CH_2Cl_2) $[M+H^+](C_{52}H_{35}O_{79}Br_4Ge_2)$: m/z Calculated : 1138.78394, m/z Found : 1138.7835 (0 ppm). 2,2 bipyridine (59 mg, 0.326 mmol, 4 eq) is added and then dissolved in 200 mL of THF. The mixture is bubbled with argon during 20 min. Degazed COD (0.04 mL, 0.326 mmol, 4 eq) and $Ni(COD)_2$ (90 mg, 0.326 mmol, 4 eq) are added and the mixture is stirred 1 night to 25°C. Then MeOH (10 mL) are added and the mixture is filtered on $MgSO_4$, washed with water and the solvent is evaporated. The crude mixture was purified by silica gel chromatography using DCM/AcOEt (8/2) to afford **15** as yellowish oil. (40 mg, η = 60 %). ^1H NMR (400 MHz, CD_2Cl_2) δ 8,04 (m, 4H, H_8), 7.94 (m, 8H, $H_{6,2or4}$), 7.56 (m, 8H, $H_{3,7}$), 7.3 (m, 6H, $H_{para,ortho}$), 7.27 (m, 8H, $H_{2or4,meta}$). ^{13}C NMR (101 MHz, CD_2Cl_2) δ 143.1 (s, 3C, C_q), 136.8 (s, C_q), 135.5 (s, C_{2or4}), 134.72 (s, C_{2or4}), 133.78 (s, C_q), 133.76 (s, C_{ortho}), 131.68 (s, C_8), 130.08 (s, C_{para}), 130.01 (s, C_{meta}), 128.60 (s, C_6), 126.18 (s, C_3), 125.46 (s, C_7). HRMS : (ESI, CH_2Cl_2) $[M+H^+](C_{52}H_{35}OGe_2)$: m/z Calculated : 823.1106, m/z Found : 823.1111.

ACKNOWLEDGMENTS

This work is supported by the Ministère de la Recherche et de l'Enseignement Supérieur, the CNRS, the Région Bretagne, the French National Research Agency (ANR Heterographene ANR-16-CE05-0003-01).

REFERENCES

(1) (a) L. Chen, Y. Hernandez, X. Feng, K. Müllen, K. *Angew. Chem. Int. Ed.* **2012**, *51*, 7640–7654. (b) A. Narita, X.-Y. Wang, X. Feng, K. Müllen, *Chem. Soc. Rev.* **2015**, *44*, 6616–6643. (c) Y. Sakamoto, T. Suzuki, *J. Am. Chem. Soc.* **2013**, *135*, 14074–14077. (d) S. Kumar, Y. -T. Tao, Y. *Org. Lett.* **2018**, *20*, 8, 2320-2323 (e) K. Kato, H.-A. Lin, M. Kuwayama, M. Nagase, Y. Segawa, L. T. Scott, K. Itami, *Chem. Sci.* **2019**, *10*, 9038–9041.

(2) K. Kawasumi, Q. Zhang, S. Segawa, L. T. Scott, K. Itami, *Nat. Chem.* **2013**, *5*, 739–744.

(3) (a) X.-Y. Wang, X. Yao, A. Narita, K. Müllen, *Acc. Chem. Res.* **2019**, *52*, 2491–2505. (b) Y. Sasaki, M. Takase, T. Okujima, S. Mori, H. Uno, *Org. Letters* **2019**, *21*, 1900–1903. (c) B. He, J. Dai, D. Zherebetskyy, T. Chen, B. A. Zhang, S. J. Teat, Q. Zhang, L. Wang, Y. Liu, *Chem. Sci.* **2015**, *6*, 3180–3186. (d) M. Stępień, E. Gońka, M. Żyła, N. Sprutta, *Chem. Rev.* **2017**, *117*, 3479–3716; (e) T. Baumgartner, F. Jaekle, (Eds), Main Group Strategies toward Functional Hybrid Materials, **2018**, John Wiley & Sons (UK), (f) P.-A. Bouit, A. Escande, R. Szűcs, D. Szieberth, C. Lescop, L. Nyulászi, M. Hissler, R. Réau, *J. Am. Chem. Soc.* **2012,** *134* (15), 6524-6527.

(4) (a) He, J. Borau-Garcia, A. Y. Y. Woo, S. Trudel, T. Baumgartner, *J. Am. Chem. Soc.* **2013**, *135*, 1137-1147 (b) Y. Ren, M. Sezen, F. Guo, F. Jäkle, Y.-L. Loo, *Chem. Sci*. **2016**, *7*, 4211-4219 (c) W. Winter, *Chem. Ber*. **1976**, *109*, 2405-2419 (d) D. Wu, C. Hu, L. Q, Z. Duan, F. Mathey *Eur. J. Org. Chem*. **2019**, *27*, 6369-6376 (e) T. Delouche, A. Mocanu, T. Roisnel, R. Szűcs, E. Jacques, Z. Benkő, L. Nyulászi, P.-A. Bouit, M. Hissler, Org. Lett. 2019, *21*, 802-806 (f) L. Wang, J. Ma, E. Si, D. Zheng, *Synthesis* **2020**, 10.1055/s-0040-1705946. (g) Y. Liu, K. Zhang, R. Tian, Z. Duan, F. Mathey, *Org. Letters* **2020**, 22, 6972-6976

(5) L. Dobelmann, A. H. Parham, A. Büsing, H. Buchholz, B. König, *RSC Adv.*, **2014**, *4*, 60473–60477.

(6) K. Schickedanz, J. Radtke, M. Bolte, H.-W. Lerner, M. Wagner, *J. Am. Chem. Soc.*, **2017**, *139*, 2842–2851.

(7) S. Hayakawa, A. Kawasaki, Y. Hong, D. Uraguchi, T. Ooi, D. Kim, T. Akutagawa, N. Fukui, H. Shinokubo, *J. Am. Chem. Soc.*, **2019**, *141*, 19807–19816.

(8) T. Delouche, R. Mokrai, T. Roisnel, D. Tondelier, B. Geffroy, L. Nyulászi, Z. Benkő, M. Hissler, P.-A. Bouit, *Chem. Eur. J.* **2020**, *26*, 1856–1863.

(9) Alternative route toward naphthyl-fused phosphepine and phosphepine oxide**:** (a) S. Zhang, X. Chu, T. Li, Z. Wang, B. Zhu, *ACS Omega* **2018** *3* (4), 4522-4533, (b) E. Regulska, H. Ruppert, F. Rominger, C. Romero-Nieto, *J. Org. Chem.* **2020**, *85*, 1247-1252.

(10) J. Hassan, M. Sévignon, C. Gozzi, E. Schulz, M. Lemaire, *Chem. Rev.* **2002**, *102*, 1359–1470.

(11) For example of Cu-catalyzed O-arylation, see: Y. Wang, C. Zhou, R. Wang, *Green Chem.* **2015**, *17*, 3910

(12) F. R. Knight, A. L. Fuller, A. M. Z. Slawin, D. Woollins, *Polyhedron* **2010**, *29*, 1849

(13) F. Riobé, R. Szűcs; C. Lescop; R. Réau; L. Nyulászi; P.-A. Bouit; M. Hissler, *Organometallics* **2017**, 36, 2502-2511.

(14) (a) V. Lyaskovskyy, R. J. A. van Dijk-Moes, S. Burck, W. I. Dzik, M. Lutz, A. W. Ehlers, J. C. Slootweg, B. de Bruin, K. Lammertsma, Organometallics, **2013**, *32*, 363–373 (b) P. S. Pregosin, *Chem. Commun*., 2008, *40*, 4875–4884.

(15) The formation of such Ge-O-Ge bond has already been described: M. Mastroianni, W. Zhu, M. Stefanelli, S. Nardis, F. R. Fronczek, K. M. Smith, Z. Ou, K. M. Kadish, R. Paolesse, *Inorg. Chem.*, **2008**, *47*, 11680–11687. A. E. Wetherby, L. R. Goeller, A. G. DiPasquale, A. L. Rheingold, C. S. Weinert, *Inorg. Chem.*, **2007**, *46*, 7579–7586. R. A. Green, C. Moore, A. L. Rheingold, C. S. Weinert, *Inorg. Chem.*, **2009**, *48*, 7510–7512.

(16) K. Padberg, J. D. R. Ascherl, F. Hampel, M. Kivala, *Chem. Eur. J.* **2020**, *26*, 3474-3478

(17) H. Maeda, T. Maeda, K. Mizuno, *Molecules* **2012**, *17*, 5108-5125.
(18) (a) J. P. Green, J. A. L. Wells, A. Orthaber, *Dalton Trans*. **2019**, 48, 4460-4466. (b) S. M. Parke, M. P. Boone, E. Rivard, *Chem. Commun*. **2016**, 52, 9485-9505.